

# Kinetics of the helix-coil transition

Armen E. Allahverdyan,<sup>1</sup> Sasun G. Gevorgian,<sup>1</sup> Aleksandr Simonian<sup>2</sup>

<sup>1</sup> Yerevan Physics Institute, Alikhanian Brothers Street 2, Yerevan 375036, Armenia

<sup>2</sup> Materials Research and Education Center, 275 Williamore Auburn University, Auburn AL 36849-5341

PACS 36.20.-r { Macromolecules and polymer molecules  
PACS 36.20.Ey { Conformation (statistics and dynamics)  
PACS 05.20.Dd { Kinetic theory

**Abstract.** – Based on the Zimm-Bragg model we study cooperative helix-coil transition driven by a finite-speed change of temperature. There is an asymmetry between the coil  $\rightarrow$  helix and helix  $\rightarrow$  coil transition: the latter is displayed already for finite speeds, and takes shorter time than the former. This hysteresis effect has been observed experimentally, and it is explained here via quantifying system's stability in the vicinity of the critical temperature. A finite-speed cooling induces a non-equilibrium helical phase with the correlation length larger than in equilibrium. In this phase the characteristic length of the coiled domain and the non-equilibrium specific heat can display an anomalous response to temperature changes. Several pertinent experimental results on the kinetics helical biopolymers are discussed in detail.

Biopolymers carry information which is embedded not only in the linear sequence of the monomers, but also in the conformational structures [1]. These structures are determined by the sequence, but they also adjust to environmental conditions. A pertinent example is the helix-coil transition (HCT), which denotes the disruption of the ordered conformation [e.g., the  $\alpha$ -helix of proteins or the triple-helix of collagen] to form a disordered coil [1]. This order-disorder transition occurs when the temperature is raised or a chemical denaturant is added.

The importance of helices in biopolymers motivated many studies on thermodynamic and kinetic aspects of HCT [1,6,9,10]. The basic model in this field was proposed by Zimm and Bragg (ZB) and successfully applied for describing the HCT both in [1,5] and out [6,12] of equilibrium. The virtue of the model is the simplicity of its ingredients: cooperativity and the free-energy preference to form a helix. Many studies devoted to the kinetics of the HCT concentrate on the relaxation from a non-equilibrium state, which is prepared experimentally via, e.g., laser-induced temperature jump [10]. This setup is adequate for small globular proteins whose relaxation time is short. The situation is different for HCT in collagen [13,16], which has very long relaxation times to equilibrium (hours and days), so that the HCT has to be probed by necessarily finite-rate temperature changes, and the very description of the HCT has to be essentially kinetic [16] (the equilibrium HCT still exists at unrealistic

long times [15]). Kinetic effects are also encountered in HCT for DNA [17,18] and for crystals of globular proteins, where each site of the crystal contains one protein [20]. This ordered protein ensemble amplifies memory and hysteresis effects and allows their clear experimental identification [20].

These experimental set-ups call for a unifying theoretical approach. Here we study the helix-coil kinetics of ZB model driven by finite-speed temperature changes. We reproduce and explain several basic experimental findings, and also predict new effects. Conceptually, there is an even deeper interest in the kinetics of the basic ZB model, since the stability of many proteins does have both kinetic and thermodynamic aspects [21].

In the ZB model one assigns the spin variable  $s_i = 1$  ( $s_i = 0$ ) for the  $i$ 'th helix (coiled) region of the polymer, and assumes the following free energy for the spins [1,2]

$$F[s] = -J \sum_{i=1}^{N-1} s_i s_{i+1} - h(T) \sum_{i=1}^N s_i; \quad (1)$$

where  $s = (s_1, \dots, s_N)$ ,  $N$  is the total number of regions, and  $J > 0$  stands for the cooperative interaction [19]. The mechanisms of cooperativity for the main biopolymers ( $\alpha$ -helices, DNA, collagen, etc) are reviewed in [1,2,14].

The term  $h(T)$  in (1) is the free energy difference of fast atomic variables in region  $i$ , calculated for a fixed value of the slow spin  $s_i$  [27]. We thus assume time-scale separation [9,10]: the joint probability  $P(s; a)$  of fast ( $a$ )

and slow (s) variables factorizes as  $P(s)P_{eq}(a|s)$ , where the conditional probability  $P_{eq}(a|s)$  is always (also for kinetic processes) at equilibrium with the bath temperature  $T$  [27]. The dynamics of the spins is then governed by the free energy (1), where  $h(T)$  favors helix (coil) formation at low (high)  $T$ :  $h(T_c) = 0$  at the equilibrium HCT temperature  $T_c$ , while  $h(T) > 0$  ( $h(T) < 0$ ) for  $T < T_c$  ( $T > T_c$ ). Experiments and ab initio calculations are consistent with a linear change of  $h(T)$  in the vicinity of  $T_c$  ( $\gamma > 0$  is a constant and  $k_B = 1$ ) [14]:

$$h(T) = (T_c - T): \quad (2)$$

The interaction strength in the model is characterized by  $\beta = e^{4J/T_c}$  [2]. In the highly-cooperative regime  $\beta \gg 1$  the equilibrium helix-coil transition resembles a real phase-transition, which combines the features of first-order (jumping order parameter) and the second-order (large correlation length) phase transitions [1,2,31].

The ZB model was originally proposed for describing the helix-coil transition in polypeptides and proteins [1,2]. Later on the equilibrium ZB model was successfully applied to the duplex-coil transition in DNA [31] and to some aspects of the triplex-coil transition in collagen [14]. In the latter two cases the ZB model is regarded as a skeletal model producing important qualitative conclusions. The purpose of this Letter is to understand the basic physics of hysteresis and memory effects during the helix-coil transition in terms of the ZB model.

Now the system described by (1) interacts with a bath at temperature  $T$ . We assume that the elementary bath-driven process amounts to local disruption (or creation) of a single helix:  $s_j \rightarrow s_j$  (spin-flipping), and that the dynamics is given by the following master equation [22]:

$$P(s;t) = \sum_{j=1}^N [P(s_j;t)w(s_j) - P(s;t)w(s_j)]; \quad (3)$$

where  $s_j = (s_1; \dots; s_{j-1}; s_j; s_{j+1}; \dots; s_N)$ ,  $P(s;t)$  is the time-dependent probability of  $s = (s_1; \dots; s_N)$ ,  $P = \partial P / \partial t$ , and where the first (second) term in the RHS of (3) describes the in- (out-) flow of probability to the configurations due to spin-flipping.  $w(s_j)$  is the transition rate  $s_j \rightarrow s_j$  which is standardly taken in the Glauber form [22]:  $w(s_j) = \frac{1}{2} [1 - s_j \tanh(\gamma_j)]$ , where  $\gamma$  is the relaxation frequency,  $\gamma = 1/T$  and  $\gamma_j = h + J(s_{j-1} + s_{j+1})$  is the local field acting on  $s_j$ ; see (1). Thus the spin-flip is probable if it decreases  $F$ . This ensures relaxation to the equilibrium  $P_{eq}[s] / e^{-F[s]}$  for a constant  $T$  [22].

Note that the spin-flipping can occur anywhere in the chain. Thus, the studied kinetics of the ZB model differs from the zipper kinetics [8,11,12,17], where the disruption of the helix can occur only at the end-points of the chain. The zipper kinetics is expected to be valid for relatively short chains, undergoing relaxation from the completely helical to the completely coiled chains [8]. Here we consider long chains.

Let us introduce the following averaged quantities:

$$m(t) = \langle s_i \rangle; \quad \langle s_{i+1} \rangle; \quad \langle s_{i+2} \rangle; \quad (4)$$

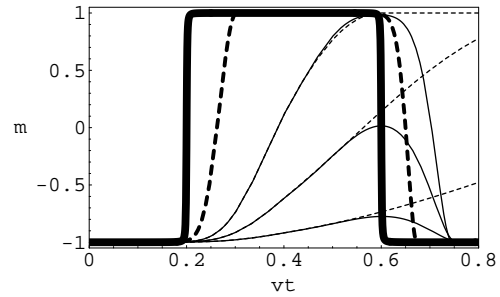


Fig. 1: The order parameter  $m$  versus dimensionless time  $vt$  under cooling-reheating with temperature speed  $v$  and parameters (10), except that  $\beta = 1.2 \cdot 10^6$ . Cooling starts at  $vt = 0$  and changes to reheating at  $vt = 0.4$ . The equilibrium  $T_c$  is crossed for  $vt = 0.2$  and  $t = 0.6$ . Thick curve: equilibrium  $m_{eq}$ , which changes between  $m_{eq} = -1$  (coil) and  $m_{eq} = 1$  (helix). Thick dashed curve:  $v = 2 \cdot 10^{-6}$ . Normal curves (from bottom to top):  $v = 5 \cdot 10^{-5}; 2 \cdot 10^{-5}; 10^{-5}$ . The dashed counterpart of each normal curve refers to cooling from  $vt = 0$  till  $vt = 0.4$ , and then holding  $T$  constant.

where  $\langle \cdot \rangle_t$  is the average over  $P(s;t)$ , while  $\frac{1+m}{2}$  is the fraction of helical regions. For  $N \gg 1$  (long chain) the boundary effects are neglected, all spins are equivalent, and (3, 4) imply

$$\dot{m} = (1 - \alpha)m + \frac{a_0}{2} + \frac{a_2}{2} \alpha; \quad (5)$$

$$\dot{\alpha} = \frac{1}{2} + \alpha + (a_0 + a_2)m + a_1 \alpha; \quad (6)$$

$$a_1 = \gamma; \quad a_{0,2} = \tanh(\gamma) + \gamma; \quad (7)$$

where  $\alpha = \frac{1}{2} \tanh(\gamma - 2J)$ . Eqs. (5, 6) are first two equations of the infinite hierarchy of moment equations. For  $h = m = 0$  this hierarchy is exactly solvable [22]. For  $h \neq 0$ , there is no exact solution, and one has to rely on approximations [6,9].

The spin-temperature ansatz amounts to assuming that the probability  $P(s;t)$  has a locally Gibbsian form with two time-dependent parameters  $\alpha_1$  and  $\alpha_2$  [23,24]:

$$P(s;t) \propto \exp[\alpha_1(t) \sum_i s_i s_{i+1} + \alpha_2(t) \sum_i s_i]; \quad (8)$$

This amounts to expressing the term  $\alpha_2$  in (5, 6) via  $\alpha_1$  and  $m$  by means of equilibrium formulas [24]

$$\alpha_k = m^2 + (1 - m^2)^{1-k} (m^2)^k; \quad k = 2; 3; \dots \quad (9)$$

Thus we assume that the higher-order moments  $\alpha_k$  relax to the local equilibrium (9), before  $m(t)$  and  $\alpha_1(t)$  relax to equilibrium [7,23,24]. Eqs. (5, 6) with  $\alpha_2$  given by (9) is now a closed pair of equations that reproduces exactly the equilibrium limit. Eqs. (5, 9) are consistent with the above-mentioned exact solution for  $h = m = 0$ , since they correctly predict the diverging relaxation time for  $J \rightarrow 1$ , as well as the transition from the exponential to a power-law decay [24]. The reliability of the spin-temperature ansatz is confirmed by its applications

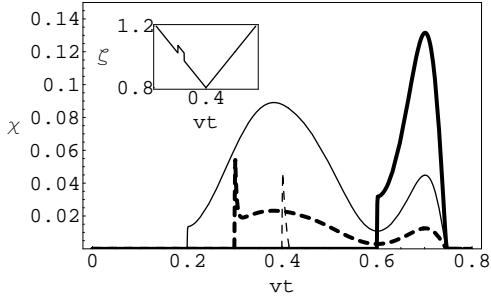


Fig. 2: Susceptibility  $\chi(t; t^0)$  versus  $vt$  under cooling-reheating with parameters (10), except that  $\beta = 1.2 \cdot 10^6$  and  $v = 10^{-5}$ . The temperature perturbation  $T_c [T_c^0 + \frac{\Delta T}{2}] [T_c^0 + \frac{\Delta T}{2}]$  has magnitude  $\Delta T = 0.001$  and is centered at  $T_c^0$ . Normal curve:  $\beta = 0.2$ ; thick-dashed:  $\beta = 0.3$ ; dashed:  $\beta = 0.41$ ; thick:  $\beta = 0.6$ . Insert: the temperature profile  $T(vt) = T_c(vt) + \Delta T$  perturbed at  $vt = 0.2$ .

in NMR/ESR physics [23,24]. For the derivations of (8) via the projection-operator method see [25].

The equilibrium  $m$  is obtained from putting to zero the LHS of (5, 6) with  $\beta$  given by (9):  $m_{eq} = \sinh(h) [\sinh^2(h) + e^{4\beta}]^{-1/2}$ . In the cooperative regime  $\beta \gg 1$ ,  $m_{eq}$  shows a sharp transition from  $m_{eq} = 0$  (coil) to  $m_{eq} = 1$  (helix) [1]; see Fig. 1.

Note that for  $h = 0$  (right at  $T = T_c$ ) (5, 7) predict that the relaxation time of  $m(t)$  is  $\frac{1}{(1 - a_1)} = \frac{1}{2}$ . This agrees with the known result [6] and shows that the relaxation time is larger for more cooperative transitions and for lower temperatures. These aspects were numerously confirmed in simulations [12].

Now assume that the bath temperature  $T(t) = T_c - \beta_0 vt$  decreases with speed  $v$  from a higher temperature  $T_{c0} > T_c$  (at which the system was equilibrated) to a lower temperature  $T_{c1} < T_c$ . Then  $T(t)$  increases back to  $T_{c0}$  with the same speed (reheating):  $T(t) = T_c - \beta_0 vt$ . For identification of asymmetries in the system response, the reheating temperature profile is taken to be the mirror reflection of the cooling profile.

For concreteness the numerical solutions of (5, 6) are displayed for the dimensionless parameters [see (2)]:

$$\beta_0 = 1.2; \quad \beta_1 = 0.8; \quad \beta_2 = 0.75; \quad \beta_3 = 3.34 \cdot 10^4; \quad (10)$$

and various values of the dimensionless cooling-reheating speed  $v$ . The values of  $\beta_0$  and  $\beta_1$  correspond to the helix-coil transition in poly- $\alpha$ -benzyl-glutamate [3]. They are typical for other cooperative helix-coil transitions [4].

The order parameter  $m$  defines the helicity fraction  $\frac{1+m}{2}$ . Fig. 1 displays the non-equilibrium  $m$  versus the dimensionless time  $vt$ , as obtained from solving numerically (5, 6, 9) with the time-dependent temperature  $T(t)$ . Fig. 1 shows that for a small (but finite) speed  $v$  the transition helix  $\rightarrow$  coil during the reheating is more visible and takes shorter time than the reverse transition coil  $\rightarrow$  helix during the cooling. The same conclusion (not displayed) holds

when doing heating and then recooling. The symmetry between helix  $\rightarrow$  coil and coil  $\rightarrow$  helix is recovered in the equilibrium limit  $\beta \rightarrow \infty$ . The asymmetry also disappears in the weakly-cooperative case  $\beta \ll 1$ . This asymmetry is an example of hysteresis and it was observed experimentally for highly-cooperative HCT in collagen [13,16], crystalline proteins [20] and DNA [18].

To gain a deeper understanding of the hysteresis, let us study in more detail the system's memory. Compare the cooling-reheating behavior of  $m(t)$  with the situation, where the temperature decreases till the lowest point and is then held constant; see Fig. 1. This cooling-holding scenario produces curves which are almost identical to the cooling-reheating curves, except at the vicinity of the equilibrium reheating transition, i.e.,  $m(t)$  does not react on the reheating before the sign of  $h$  changes. Let us quantify the memory via susceptibility

$$\chi(t; t^0) = \lim_{\Delta T \rightarrow 0} [m(t) - m(t^0)] / \Delta T; \quad (11)$$

Here  $m(t)$  is obtained under the same cooling-reheating temperature setup, but  $\Delta T$  perturbed at  $t^0$ :

$$T(t) = T_c - \beta_0 vt + \Delta T [\theta(t - t^0) - \theta(t - t^0 - \Delta t)]; \quad (12)$$

where  $\theta(t)$  is the step function, and where the perturbation duration  $\Delta t$  is small but finite; see Fig. 2. The perturbation is designed such that at equilibrium, where  $m(t)$  is a function of the time-dependent temperature  $T(t)$ ,  $\chi(t; t^0)$  is non-zero only for  $v t^0 - t^0 < \Delta t$ . In the regime where the above asymmetry is present, there are basically three scenarios for the behavior of  $\chi(t; t^0)$ ; see Fig. 2. i) A perturbation introduced during the cooling in the vicinity of  $T_c$  is memorized and amplified. This memory need not be monotonic: it revives once  $T(t)$  crosses  $T_c$  during the reheating; see Fig. 2. ii) The same perturbation introduced during the reheating in the vicinity of  $T_c$  creates a stronger immediate response, but a weaker memory, as compared to the previous case. iii) Outside of the vicinity of  $T_c$  the response resembles that in equilibrium:  $\chi(t; t^0)$  is maximal for  $t^0 = t$  and quickly decays for  $|t - t^0| > 0$ ; see Fig. 2. We thus see how the hysteresis emerges from the instabilities at  $T(t) = T_c$  during the cooling and reheating.

Specific heat is a well-known indicator of the helix-coil transitions, which are observed via calorimetric methods [1]. Recalling the discussion before (2) and definitions (7), one can see that the energy of the spins is  $N u(t)$  [27], with

$$u(t) = -J(t) \langle [h(T)] m(t) \rangle; \quad (13)$$

The origin of this formula should be clear from (1, 4). Note that the term  $\langle [h(T)] \rangle$  is similar to the known equilibrium formula  $E = \langle [F] \rangle$  relating energy  $E$  to the free energy  $F$ . The specific heat  $c(t)$  is the response of  $u(t)$  to the temperature change  $[T - T] = T$ :

$$c(t) = \frac{d u(t)}{d T} = -[J_- + T m_-] = T; \quad (14)$$

The equilibrium specific heat  $c_{eq}$  is always positive and shows two sharp and symmetric peaks at  $T = T_c$ ; see

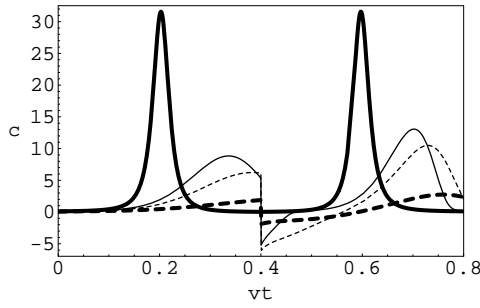


Fig. 3: Specific heat  $c$  versus the dimensionless time  $vt$  under cooling-reheating with parameters (10). Normal curve:  $v = \frac{1}{5} \cdot 10^3$ . Dashed curve:  $v = \frac{1}{3} \cdot 10^3$ . Dashed-thick curve:  $v = 10^3$ . Thick curve: equilibrium  $c_{eq}$ .

Fig. 3. For the non-equilibrium specific heat we see again the asymmetry between helix-coil and coil-helix transitions: the peak of  $c$  during cooling is either absent or less visible than the one during the reheating. Now  $c(t)$  can be negative, i.e., the internal energy can decrease upon reheating; see Fig. 3. This is partially related to the response of  $m(t)$ : Fig. 1 shows that when cooling changes to reheating,  $m(t)$  continues to increase due to its memory. In contrast,  $m_{eq}$  decreases under reheating. The negative part of  $c$  is most pronounced for a finite cooling-reheating speed  $v$ ; see Fig. 3. Note that a negative specific heat is met in glasses, within a different scenario that is also related to large relaxation times [26].

The kinetic transition temperature  $T$  can be related to the peak of the specific heat [15,16]; see Fig. 3. For not very small  $v$ ,  $T$  is approximately a linear function of  $\ln \frac{v}{2}$ ; thus  $T$  is not susceptible to moderate changes in the cooling-reheating speed  $v$ . The same scaling of the kinetic transition temperature was seen experimentally for the helix-coil transition of collagen [15]. For the parameters of Fig. 3 we obtained  $(T_{C,R} - T_c) = T_c = a_{C,R}x + b_{C,R}$  for  $x \in [2; 3.5]$ . Here the lower indices C and R refer to the cooling and reheating, respectively, while  $a_R = 0.09$ ,  $a_C = 0.12$ ,  $b_R = 0.32$ , and  $b_C = 0.41$ . We see that  $T_R > T_C > T_c$ .

The correlation function  $g(k;t) = \langle h_{i_1} s_{i_1+k} i_t h_{i_1} i_t h_{i_1+k} i_t \rangle$  describes the spatial structure of fluctuations. Eq. (9) implies  $g(k;t) = [1 - m^2(t)] e^{-k^2 \xi(t)}$ , where

$$\xi(t) = \ln \frac{1 - m^2(t)}{(t) - m^2(t)}; \quad (15)$$

is the correlation length, or the cooperative unit length, which plays an important role in describing the cooperativity of the polymer structure [1]. The equilibrium  $\xi_{eq}$ , obtained from (15) by  $m(t) \rightarrow m_{eq}$  and  $(t) \rightarrow \xi_{eq}$ , displays two sharp peaks at  $T = T_c$ ; see Fig. 4. It directly relates to the cooperativity parameter:  $\xi_{eq}(T = T_c) = \frac{1}{2} \frac{1}{1 - m_{eq}^2}$  [1].  $\xi_{eq}$  is small both below and above  $T_c$ , since there are not much equilibrium fluctuations there.

The non-equilibrium behavior of  $\xi(t)$  is different: for

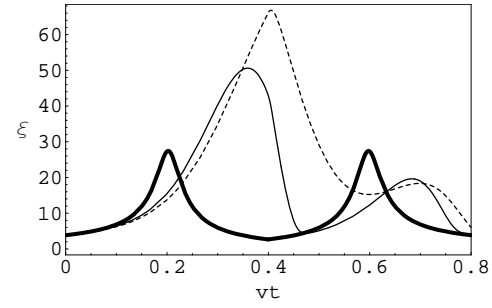


Fig. 4: Correlation length  $\xi$  versus  $vt$  under cooling-reheating with parameters (10). Normal curve:  $v = \frac{1}{5} \cdot 10^3$ . Dashed curve:  $v = \frac{1}{3} \cdot 10^3$ . Thick curve: equilibrium  $\xi_{eq}$ .

finite speeds  $\xi(t)$  increases during cooling, and its maximum is reached for the lowest  $T$ ; see Fig. 4.  $\xi(t)$  is maximal at a certain finite speed of the cooling-reheating. Around its maximum it is larger than  $\xi_{eq}(T = T_c)$ . Thus the equilibrium relation between step-like change of the order parameter and the correlation length is broken in kinetics: now  $m(t)$  does not show transition during cooling, but  $\xi(t)$  is large. The reason for a large  $\xi(t)$  is that the spin-spin interaction energy  $\langle h_i h_{i+k} \rangle$  is close to 1 for both  $T < T_c$  and  $T > T_c$ , while  $m(t)$  is far from 1; see (45) and Fig. 1. Thus there are many helical and coiled domains, whose total spin should sum to zero implying long correlations. Yet another interpretation of a large  $\xi(t)$  is that due to memory the system does not see the sign change of  $h(T)$ , but it sees the lowering of  $T(t)$ , which naturally increases its correlation length  $\xi(t)$ . Thus the finite-rate cooling plays a selective role suppressing one mechanism and activating another. In the non-cooperative case  $\beta \rightarrow 1$ ,  $\xi(t)$  follows to the shape of  $\xi_{eq}$ , and  $\xi(t) < \xi_{eq}$  for all temperatures.

Domain lengths. Generally, the state of the studied linear polymer is inhomogeneous and consists of helical and coiled domains. To characterize the domain lengths, we consider the probability  $P(k) = \sum_{j=1}^Q \frac{1}{2} \frac{s_j}{t}$  of having a helical ( $P_+$ ) or coiled ( $P_-$ ) domain of length  $k$ . The transfer matrix treatment of (8) leads to  $P(k) = e^{-k^2 \xi(t)}$ , where  $\xi(t)$  does not depend on  $k$ . Thus,  $e^{-1} = P(2) = P(1)$ , or

$$\xi(t) = \ln \frac{2 - 2m(t)}{1 + (t) - 2m(t)}; \quad (16)$$

where  $\xi_+$  and  $\xi_-$  are, respectively, the characteristics length of the helical and coiled domains. Naturally, the equilibrium  $\xi_{eq}$  is large in the coiled phase and decreases under cooling becoming small in the helical phase; see Fig. 5. Likewise,  $\xi_+$  is large (small) in the helical (coiled) phase. Note that  $\xi_+(T_c) = \xi_-(T_c)$ . In contrast to the equilibrium  $\xi_{eq}$ , we see in Fig. 5 that  $\xi(t)$  can increase in time, if the cooling is not very slow. It decreases once the reheating starts. Thus  $\xi(t)$  reacts stronger on the decrease of temperature, than on changing the sign of  $h$ . Since during the cooling the order parameter  $m$  increases,

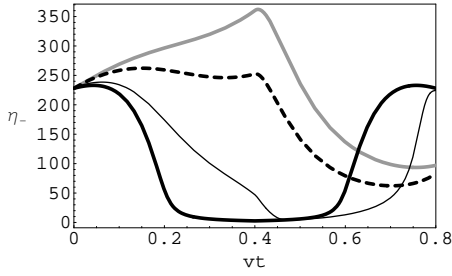


Fig. 5: The coiled domain length  $\eta_-$  versus  $vt$  under cooling-reheating with parameters (10). Gray curve:  $v = \frac{1}{5} \cdot 10^{-2}$ . Thick-dashed curve:  $v = 10^{-3}$ . Normal curve:  $v = \frac{1}{5} \cdot 10^{-3}$ . Thick curve: equilibrium  $\eta_{-,eq}$ .

we see that the number of helical segments increases, but the typical coiled domain gets larger. Fig. 5 also shows that  $\eta_-$  can behave non-monotonically with time. For very small speeds,  $\eta_-$  reproduces (with a delay) the shape of  $\eta_{-,eq}$ ; see Fig. 5. The behavior of  $\eta_+$  (t) under cooling-reheating is less interesting: it follows, in a delayed and weakened form, the shape of  $\eta_{+,eq}$ ; see Fig. 6. (The same conclusion holds for  $\eta_+$  during the heating from  $T < T_c$  and then recooling.) Note that for finite speeds we can have  $\eta_+ > \eta_-$  at low temperatures; see Figs. 5, 6.

**Relations with experiments.** We now discuss several experimental results on helical biopolymers that demonstrate clear signs of irreversibility and hysteresis.

Admittedly, many experiments in polypeptides and proteins do not show visible signs of memory and hysteresis (unless caused by irreversible aggregation), mainly because the experimental temperature changes are too slow compared to relevant relaxation times [21].

However, there are susceptible experiments on crystals of globular proteins, which do show memory effects during various conformational changes [20]. Here each site of the crystalline structure contains one protein. Memory effects are amplified by this ordered structure and are visible in experiments [20]. Along these lines, we present here several new experimental results. Note that irreversibilities and hysteresis effects here are not associated with the crystalline structure *per se* [20]; they are related to helix-coil features proteins, while the crystalline structure only serves for amplifying these effects.

Fig. 7 shows the denaturation process for crystalline protein A boohold dehydrogenase. The process is monitored via the change of the Young's modulus with temperature. Recall that the Young's modulus is defined as the ratio of the applied stress [pressure] over the induced strain. The Young's modulus serves as an indicator of structural transitions [28,29], since in the denaturated state it is smaller than in the native state. The Young's modulus of an A boohold dehydrogenase sample was measured via analyzing the electrically excited transverse resonance vibrations of the sample, which is cantilevered from one edge (another edge is free) [28,29]. The denaturation temperature of A boohold

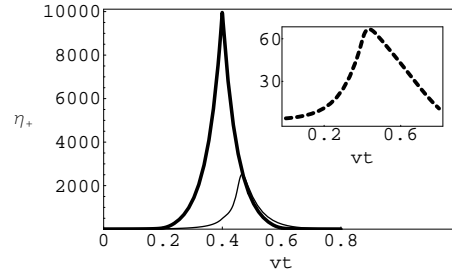


Fig. 6: The helical domain length  $\eta_+$  versus the dimensionless time  $vt$  under cooling-reheating with parameters (10). Normal curve:  $v = \frac{1}{5} \cdot 10^{-3}$ . Thick curve: equilibrium  $\eta_{+,eq}$ . Insert: the same with  $v = 10^{-3}$ .

Dehydrogenase ( $T_c \approx 45.5^\circ\text{C}$ ) is identified via the sudden jump of the Young modulus; see Fig. 7. This agrees with the denaturation temperature obtained via calorimetric methods [30].

Fig. 7 shows that once the heating is substituted by re-cooling in the vicinity of the critical temperature, the system follows a different path (hysteresis), although the heating-re-cooling speed was rather small. Moreover, even though the heating has been changed to re-cooling, the Young modulus keeps on decreasing till  $40^\circ\text{C}$  due to the memory on the previous heating stage; see Fig. 7. These effects agree qualitatively with the theoretical results found above via Zimm-Bragg model.

In contrast to polypeptides and proteins, there are established experimental results concerning the hysteresis and memory effects for DNA [17,18] and collagen [13,16]. In both these biopolymers the helical state (duplex for DNA and triplex for collagen) is stabilized by inter-molecular (i.e., inter-strand) interactions.

Fig. 8 displays the experimental denaturation of an amorphous DNA film. The same effects of hysteresis and memory are present here. For other experimental indications of memory and hysteresis effects during DNA denaturations see Refs. [18]. Ref. [31] critically assesses the applicability of the Zimm-Bragg model to the helix-coil transition in DNA, and finds that many experimental aspects of this complex phenomenon are adequately reflected in the equilibrium Zimm-Bragg model.

Ref. [14] investigates the equilibrium Zimm-Bragg model in the context of the helix-coil transition in collagen III. For this biopolymer the end-points of the three strands are held together by disulfide bonds, which precludes mismatches during the renaturation and makes possible the application of the Zimm-Bragg model. Indeed, it was found that although experimentally the helix-coil transition in collagen III (as well as in collagen I) is always kinetic [the proper equilibrium regime is hardly reached within the experimental observation time] some important aspects of the phenomenon can be described within the equilibrium Zimm-Bragg model in quantitative agreement with experiments [14]. We thus expect that the ki-

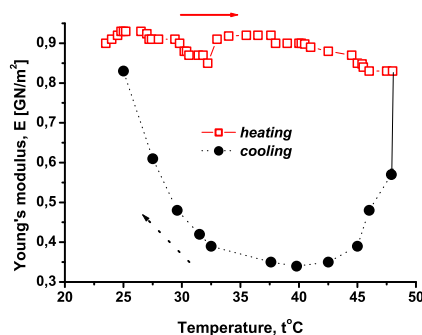


Fig. 7: The Young modulus versus temperature for a rhombohedral crystal (direction  $[z]$ ) each site of which contains a lo-hold dehydrogenase protein. Molecular weight of this protein is 80 kDa. The relative humidity is 97 % at 25 °C. The water content at this temperature is 0.37 g of water per 1 g of dry protein. The speed of heating/recooling is 0.1 °C per minute.

netics of the Zimm-Bragg model can describe the qualitative aspects of memory and hysteresis.

In sum, based on the Zimm-Bragg model we studied kinetics of the helix-coil transition driven by a finite-speed temperature change. We reproduced well-known experimental results on the hysteresis during the kinetic transition and explained it by quantifying the process memory. We also predicted new scenarios of kinetic helix-coil transition related to i) negative non-equilibrium specific heat accompanying the hysteresis; ii) correlation length becoming larger than in equilibrium.

There is an increasing evidence that the characteristics of many important biopolymers is controlled by both kinetic and thermodynamic factors [21]. For instance, the helix-coil transitions in collagen are normally kinetic, because the equilibrium is not reached within reasonable times. Moreover, the kinetic helix-coil transition temperature of collagen for various organisms is close to their physiological temperature [15], since this kinetic transition plays a role in achieving the flexibility of the collagen fiber [15]. Since our results indicate on new scenarios of kinetic helix-coil transitions in the basic Zimm-Bragg model, they can be relevant for understanding the interplay between the kinetics and thermodynamics in biopolymers.

A. A. thanks Y. M. Masakhlisov for discussions. The work was supported by Volkswagenstiftung, ANSEF and SCS of Armenia (grant 08-0166).

## REFERENCES

- [1] K. Sneppen and G. Zocchi, *Physics in Molecular Biology* (Cambridge University Press, Cambridge, 2005).
- [2] H. Qian and J. A. Schellman, *J. Phys. Chem.* 96, 3987 (1992). A. J. D. Oig, *Biophys. Chem.* 101-102, 281 (2002).
- [3] B. H. Zimm et al., *PNAS*, 45, 1601 (1970).
- [4] M. Go et al., *J. Chem. Phys.* 52, 2060 (1970).
- [5] M. Takano et al., *J. Chem. Phys.* 116, 2219 (2002).

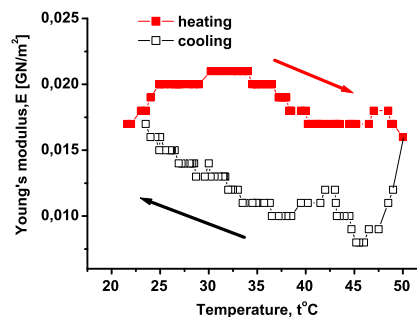


Fig. 8: The Young modulus versus temperature for an amorphous DNA film. Each DNA macromolecules (taken from a sturgeon mail) weights 1 000 kDa. The relative humidity is 95 % at 25 °C. The water content at this temperature is 0.42 g of water per 1 g of dry DNA. The speed of heating/recooling is 0.1 °C per minute.

- [6] G. Schwartz, *J. Mol. Biol.* 11, 64 (1965). D. Poland and H. A. Scheraga, *J. Chem. Phys.* 45, 2071 (1966).
- [7] H. W. Huang, *Phys. Rev. A*, 8, 2553 (1973).
- [8] T. R. Chay and C. L. Stevens, *Macromolecules*, 8, 531 (1975).
- [9] A. Baumgartner and K. Binder, *J. Chem. Phys.*, 70, 429 (1979).
- [10] M. Takano et al., *J. Chem. Phys.* 118, 10312 (2003).
- [11] D. Porschke et al., *Biopolymers*, 12, 1313 (1973).
- [12] J. Bokkyoo and D. L. Weaver, *J. Chem. Phys.*, 112, 4394 (2000).
- [13] J. M. Davis and H. P. Bachinger, *J. Biol. Chem.* 268, 25965 (1993).
- [14] J. Engeland and H. P. Bachinger, *Matrix Biol.* 19, 235 (2000).
- [15] E. Leikina et al., *PNAS* 99, 1314 (2002).
- [16] C. A. Miles, *Biopolymers*, 87, 51 (2007).
- [17] V. V. Anshelevich et al., *Biopolymers*, 23, 39 (1984).
- [18] K. E. van Holde, *Physical Biochemistry* (Prentice Hall, NJ, 1985). P. R. Bergethon, *The Physical Basis of Biochemistry* (Springer-Verlag, NY, 1998).
- [19] Note that the ZB model has several different appearances. All of them are equivalent to (1) for a long chain.
- [20] S. G. Gevorgian et al., *Eur. Biophys. J.* 34, 539 (2005).
- [21] D. Baker and D. A. Gard, *Biochemistry* 33, 7505 (1994). I. M. P. Laza del Pino et al., *Proteins* 40, 58 (2000).
- [22] R. J. Glauber, *J. Math. Phys.* 4, 294 (1963).
- [23] M. Goldman, *Spin Temperature and NMR in Solids* (Clarendon Press, Oxford, 1970).
- [24] G. O. Berim and A. R. Kessel, *Physica A* 101, 112 (1980).
- [25] J. Rau and B. Müller, *Phys. Rep.* 272, 1 (1996).
- [26] J. Bisquet, *Am. J. Phys.*, 73, 735 (2005).
- [27] A. E. A. llahverdyan and Th. M. Nieuwenhuizen, *Phys. Rev. E* 62, 845 (2000).
- [28] S. G. Gevorgian and V. N. Morozov, *Biofizika* 28, 944 (1983).
- [29] V. N. Morozov and S. G. Gevorgian, *Biopolymers* 24, 1785 (1985).
- [30] P. L. Privalov, *Adv. Prot. Chem.* 35, 1 (1982).
- [31] A. A. Vedenov et al. *Sov. Phys. Usp.* 14, 715 (1972). M. Ya. Azbel, *Phys. Rev. A* 20, 1671 (1979).